Degenerate Higgs Boson in the NMSSM near $\mathbf{125}$ GeV

Jack Gunion
U.C. Davis

Implications of LHC results for TeV-scale physics

Collaborators: Y. Jiang, S. Kraml

Higgs-like LHC Excesses at 125 GeV

- Experimental Higgs-like excesses: define

$$R_Y^h(X) = \frac{\sigma(pp \to Y \to h)\mathrm{BR}(h \to X)}{\sigma(pp \to Y \to h_{SM})\mathrm{BR}(h_{SM} \to X)}\,, \quad R^h(X) = \sum_Y R_Y^h\,, \qquad (1)$$

where $Y = gg$ or WW.

Table 1: Summary of current status for 125 GeV

$R(X)$, $X =$	$\gamma\gamma$	4ℓ	$\ell\nu\ell\nu$	$b\bar{b}$	$\tau^+\tau^-$
ATLAS	$\sim 1.9 \pm 0.5$	$\sim 1.1 \pm 0.6$	0.5 ± 0.6	0.5 ± 2.3	0.4 ± 2.0
CMS	$\sim 1.6 \pm 0.6$	$\sim 0.7 \pm 0.3$	0.6 ± 0.5	0.1 ± 0.7	$\sim 0 \pm 0.8$

In addition, we have

$$R_{WW}^{\mathrm{ATLAS}}(\gamma\gamma) = 2.5 \pm 1.2 \quad R_{WW}^{\mathrm{CMS}}(\gamma\gamma) = 2.3 \pm 1.3 \qquad (2)$$

and also there are CMS, ATLAS and D0+CDF=Tevatron measurements of Vh production with $h \to b\bar{b}$ giving at 125 GeV

$$R_{Vh}^{\rm CMS}(b\bar{b}) = 0.5 \pm 0.6\,, \quad R_{Vh}^{\rm ATLAS}(b\bar{b}) \sim 0.5 \pm 2.0\,, \quad R_{Vh}^{\rm Tev}(b\bar{b}) \sim 1.8 \pm 1\,, \tag{3}$$

all being very crude estimates read off of Friday transparencies.

Note: $R(WW) < 1$ would imply $gg \to h <$SM, but WW signal is diffuse and I will choose to mainly pay attention to $R(ZZ)$:

$R(ZZ) \gtrsim 1$ for ATLAS, whereas $R(ZZ) < 1$ for CMS.

- The big questions:
  1. if the deviations from a single SM Higgs survive what is the model?
  2. If they do survive, how far beyond our "standard" model set must we go to describe them?

Here, I focus on a particularly amusing possibility in the NMSSM: degenerate h_1 and h_2 near 125 GeV.

Enhanced Higgs signals in the NMSSM

- NMSSM=MSSM+$\widehat{S}$.

- The extra complex S component of $\widehat{S} \Rightarrow$ the NMSSM has h_1, h_2, h_2, a_1, a_2.

- The new NMSSM parameters of the superpotential (λ and κ) and scalar potential (A_λ and A_κ) appear as:

$$W \ni \lambda \widehat{S} \widehat{H}_u \widehat{H}_d + \frac{\kappa}{3} \widehat{S}^3 \,, \quad V_{\rm soft} \ni \lambda A_\lambda S H_u H_d + \frac{\kappa}{3} A_\kappa S^3 \tag{4}$$

- $\langle S \rangle \neq 0$ is generated by SUSY breakng and solves μ problem: $\mu_{\rm eff} = \lambda \langle S \rangle$.

- First question: Can the NMSSM give a Higgs mass as large as $125~\mathrm{GeV}$?

  Answer: Yes, so long as it is not a highly unified model. For this study we employ universal m_0, except for NUHM ($m^2_{H_u}$, $m^2_{H_d}$, m^2_S free), universal $A_t = A_b = A_\tau = A_0$ but allow A_λ and A_κ to vary freely.

- **Can this model achieve rates in $\gamma\gamma$ and 4ℓ that are $>$SM?**

  Answer: it depends on whether or not we insist on getting good a_μ.

- **The possible mechanism (arXiv:1112.3548, Ellwanger) is to reduce the $b\bar{b}$ width of the mainly SM-like Higgs by giving it some singlet component. The gg and $\gamma\gamma$ couplings are less affected.**

- **Typically, this requires m_{h_1} and m_{h_2} to have similar masses (for singlet-doublet mixing) and large λ (to enhance Higgs mass).**

  Large λ (by which we mean $\lambda > 0.1$) is only possible while retaining perturbativity up to m_{Pl} if $\tan\beta$ is modest in size.

  In the semi-unified model we employ, enhanced rates and/or large λ cannot be made consistent with decent δa_μ.

- **The "enhanced" SM-like Higgs can be either h_1 or h_2.**

- **Some illustrative results from JFG, Kraml, Jiang (in preparation) follow. (We focus on gg fusion here.)**

Figure Legend

	LEP/Teva	B-physics	$\Omega h^2 > 0$	$\delta a_\mu(\times 10^{10})$	XENON100	$R^{h_1/h_2}(\gamma\gamma)$
●	$\surd$	$\surd$	$0 - 0.136$	$\times$	$\surd$	$[0.5, 1]$
■	$\surd$	$\surd$	$0 - 0.094$	$\times$	$\surd$	$(1, 1.2]$
▲	$\surd$	$\surd$	$0 - 0.094$	$\times$	$\surd$	> 1.2
■	$\surd$	$\surd$	0.094-0.136	$\times$	$\surd$	$(1, 1.2]$
▲	$\surd$	$\surd$	0.094-0.136	$\times$	$\surd$	> 1.2
◆	$\surd$	$\surd$	$0.094 - 0.136$	4.27-49.1	$\surd$	~ 1

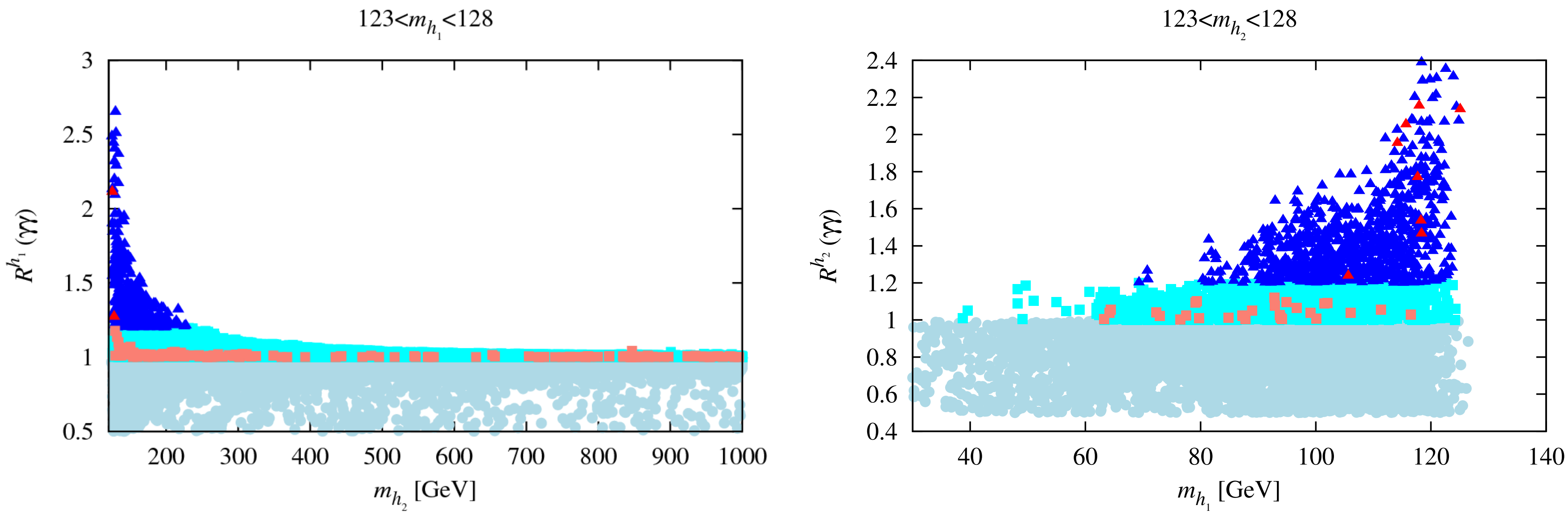

Figure 1: **The plot shows $R(\gamma\gamma)$ for the cases of $123 < m_{h_1} < 128$ GeV and $123 < m_{h_2} < 128$ GeV.**

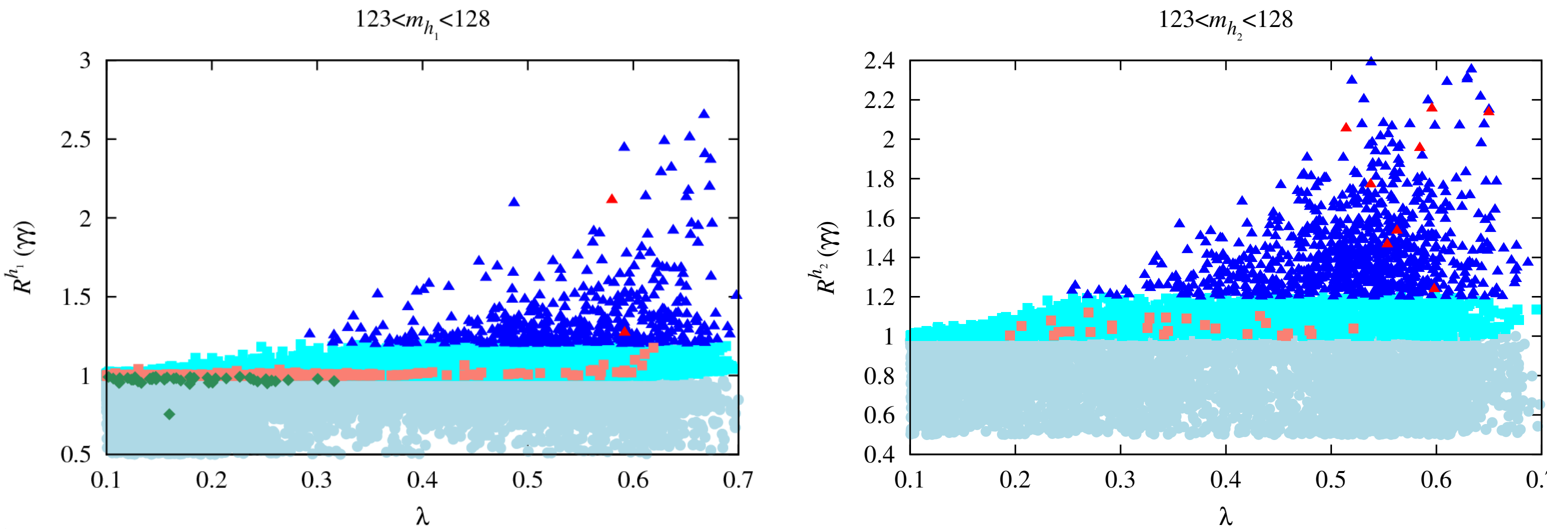

Figure 2: **Observe the clear general increase in maximum $R(\gamma\gamma)$ with increasing λ. Green points have good δa_μ, $m_{h_2} > 1$ TeV BUT $R(\gamma\gamma) \sim 1$.**

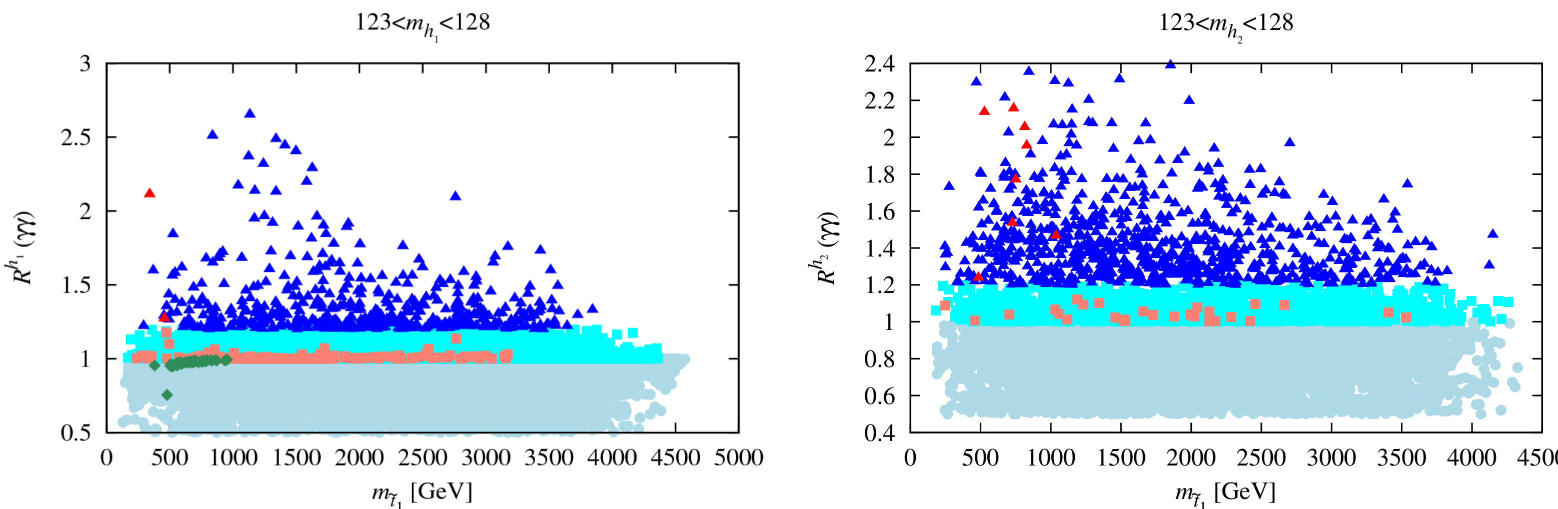

Figure 3: **The lightest stop has mass $\sim 300 - 700$ GeV for red-triangle points.**

- If we ignore δa_μ, then $R(\gamma\gamma) > 1.2$ (even > 2) is possible while satisfying all other constraints provided h_1 and h_2 are close in mass, especially in the case where $m_{h_2} \in [123, 128]~\mathrm{GeV}$ window.

- This raises the issue of scenarios in which *both* m_{h_1} and m_{h_2} are in the $[123, 128]~\mathrm{GeV}$ window where the experiments see the Higgs signal.

- If h_1 and h_2 are sufficiently degenerate, the experimentalists might not have resolved the two distinct peaks, even in the $\gamma\gamma$ channel.

- The rates for the h_1 and h_2 could then add together to give an enhanced $\gamma\gamma$, for example, signal.

- The apparent width or shape of the $\gamma\gamma$ mass distribution could be altered.

- There is more room for an apparent mismatch between the $\gamma\gamma$ channel and other channels, such as $b\bar{b}$ or 4ℓ, than in non-degenerate situation.

  In particular, the h_1 and h_2 will generally have different gg and WW production rates and branching ratios.

Degenerate NMSSM Higgs Scenarios: arXiv:1207.1545, JFG, Kraml, Yun

- **For the numerical analysis, we use NMSSMTools version 3.2.0, which has improved convergence of RGEs in the case of large Yukawa couplings.**

- **The precise constraints imposed are the following.**

1. **Basic constraints: proper RGE solution, no Landau pole, neutralino LSP, Higgs and SUSY mass limits as implemented in NMSSMTools-3.2.0.**
2. B **physics:** $\mathrm{BR}(B_s \to X_s\gamma)$, ΔM_s, ΔM_d, $\mathrm{BR}(B_s \to \mu^+\mu^-)$, $\mathrm{BR}(B^+ \to \tau^+\nu_\tau)$ **and** $\mathrm{BR}(B \to X_s\mu^+\mu^-)$ **at** 2σ **as encoded in NMSSMTools-3.2.0, plus updates.**
3. **Dark Matter:** $\Omega h^2 < 0.136$**, thus allowing for scenarios in which the relic density arises at least in part from some other source.**
   However, we single out points with $0.094 \leq \Omega h^2 \leq 0.136$**, which is the 'WMAP window' defined in NMSSMTools-3.2.0.**

4. **Xenon 100: spin-independent LSP–proton scattering cross section bounds implied by the neutralino-mass-dependent Xenon100 bound. (For points with $\Omega h^2 < 0.094$, we rescale these bounds by a factor of $0.11/\Omega h^2$.)**
5. **δa_μ ignored: impossible to satisfy for scenarios we study here.**

- **The individual h_1 and h_2 signals are:**

$$R^{h_i}_{gg}(X) \equiv \frac{\Gamma(gg \to h_i)\,\mathrm{BR}(h_i \to X)}{\Gamma(gg \to h_{SM})\,\mathrm{BR}(h_{SM} \to X)}, \tag{5}$$

$$R^{h_i}_{\mathrm{VBF}}(X) \equiv \frac{\Gamma(WW \to h_i)\,\mathrm{BR}(h_i \to X)}{\Gamma(WW \to h_{SM})\,\mathrm{BR}(h_{SM} \to X)}, \tag{6}$$

where h_i is the i^{th} NMSSM scalar Higgs, and h_{SM} is the SM Higgs boson.

Note that the corresponding ratio for $V^* \to V h_i$ ($V = W, Z$) with $h_i \to X$ is equal to $R^{h_i}_{\mathrm{VBF}}(X)$.

- **Compute the effective Higgs mass in given production and final decay** channels Y and X, respectively, as

$$m_h^Y(X) \equiv \frac{R_Y^{h_1}(X) m_{h_1} + R_Y^{h_2}(X) m_{h_2}}{R_Y^{h_1}(X) + R_Y^{h_2}(X)} \tag{7}$$

and define the net signal to simply be

$$R_Y^h(X) = R_Y^{h_1}(X) + R_Y^{h_2}(X)\,. \tag{8}$$

- The extent to which it is appropriate to combine the rates from the h_1 and h_2 depends upon the degree of degeneracy and the experimental resolution.

  Very roughly, one should probably think of $\sigma_{\rm res} \sim 1.5~{\rm GeV}$ or larger. The widths of the h_1 and h_2 are very much smaller than this resolution.

- We perform scans covering the following parameter ranges:

$$\begin{gathered} 0 \leq m_0 \leq 3000; \quad 100 \leq m_{1/2} \leq 3000; \quad 1 \leq \tan\beta \leq 40; \\ -6000 \leq A_0 \leq 6000; 0.1 \leq \lambda \leq 0.7; \quad 0.05 \leq \kappa \leq 0.5; \\ -1000 \leq A_\lambda \leq 1000; \quad -1000 \leq A_\kappa \leq 1000; \quad 100 \leq \mu_{eff} \leq 500\,. \end{gathered} \tag{9}$$

We only display points which pass the basic constraints, satisfy B-physics constraints, have $\Omega h^2 < 0.136$, obey the XENON100 limit on the LSP scattering cross-section off protons *and* have *both* h_1 and h_2 in the desired mass range: $123~\mathrm{GeV} < m_{h_1}, m_{h_2} < 128~\mathrm{GeV}$.

- In Fig. 4, points are color coded according to $m_{h_2} - m_{h_1}$.

  Circular points have $\Omega h^2 < 0.094$, while diamond points have $0.094 \leq \Omega h^2 \leq 0.136$ (*i.e.* lie within the WMAP window).

- Many of the displayed points are such that $R^{h_1}_{gg}(\gamma\gamma) + R^{h_2}_{gg}(\gamma\gamma) > 1$.

- A few such points have Ωh^2 in the WMAP window.

  These points are such that either $R^{h_1}_{gg}(\gamma\gamma) > 2$ or $R^{h_2}_{gg}(\gamma\gamma) > 2$, with the R for the other Higgs being small. Scanning is continuing.

- However, the majority of the points with $R^{h_1}_{gg}(\gamma\gamma) + R^{h_2}_{gg}(\gamma\gamma) > 1$ have $\Omega h^2 < 0.094$ and the $\gamma\gamma$ signal is often shared between the h_1 and the h_2.

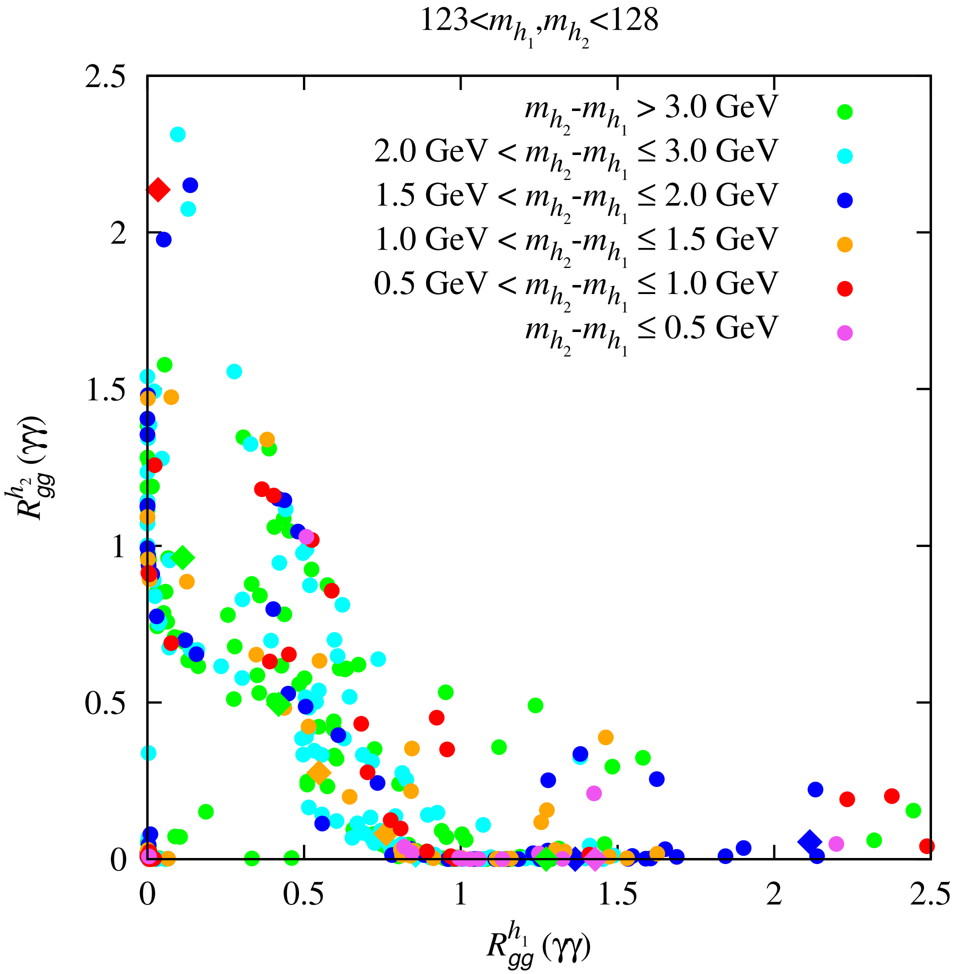

Figure 4: Correlation of $gg \to (h_1, h_2) \to \gamma\gamma$ signal strengths when both h_1 and h_2 lie in the 123–128 GeV mass range. The circular points have $\Omega h^2 < 0.094$, while diamond points have $0.094 \leq \Omega h^2 \leq 0.136$. Points are color coded according to $m_{h_2} - m_{h_1}$.

Now combine the h_1 and h_2 signals as described above. Recall: circular (diamond) points have $\Omega h^2 < 0.094$ ($0.094 \leq \Omega h^2 \leq 0.136$). Color code:

1. red for $m_{h_2} - m_{h_1} \leq 1$ GeV;
2. blue for 1 GeV $< m_{h_2} - m_{h_1} \leq 2$ GeV;
3. green for 2 GeV $< m_{h_2} - m_{h_1} \leq 3$ GeV.

- For current statistics and $\sigma_{\rm res} \gtrsim 1.5$ GeV we estimate that the h_1 and h_2 signals will not be seen separately for $m_{h_2} - m_{h_1} \leq 2$ GeV.
- In Fig. 5, we show results for $R^h_{gg}(X)$ for $X = \gamma\gamma, VV, b\bar b$. Enhanced $\gamma\gamma$ and VV rates from gluon fusion are very common.
- The bottom-right plot shows that enhancement in the Wh with $h \to b\bar b$ rate is also natural, though not as large as the best fit value suggested by the new Tevatron analysis.
- Diamond points (*i.e.* those in the WMAP window) are rare, but typically show enhanced rates.

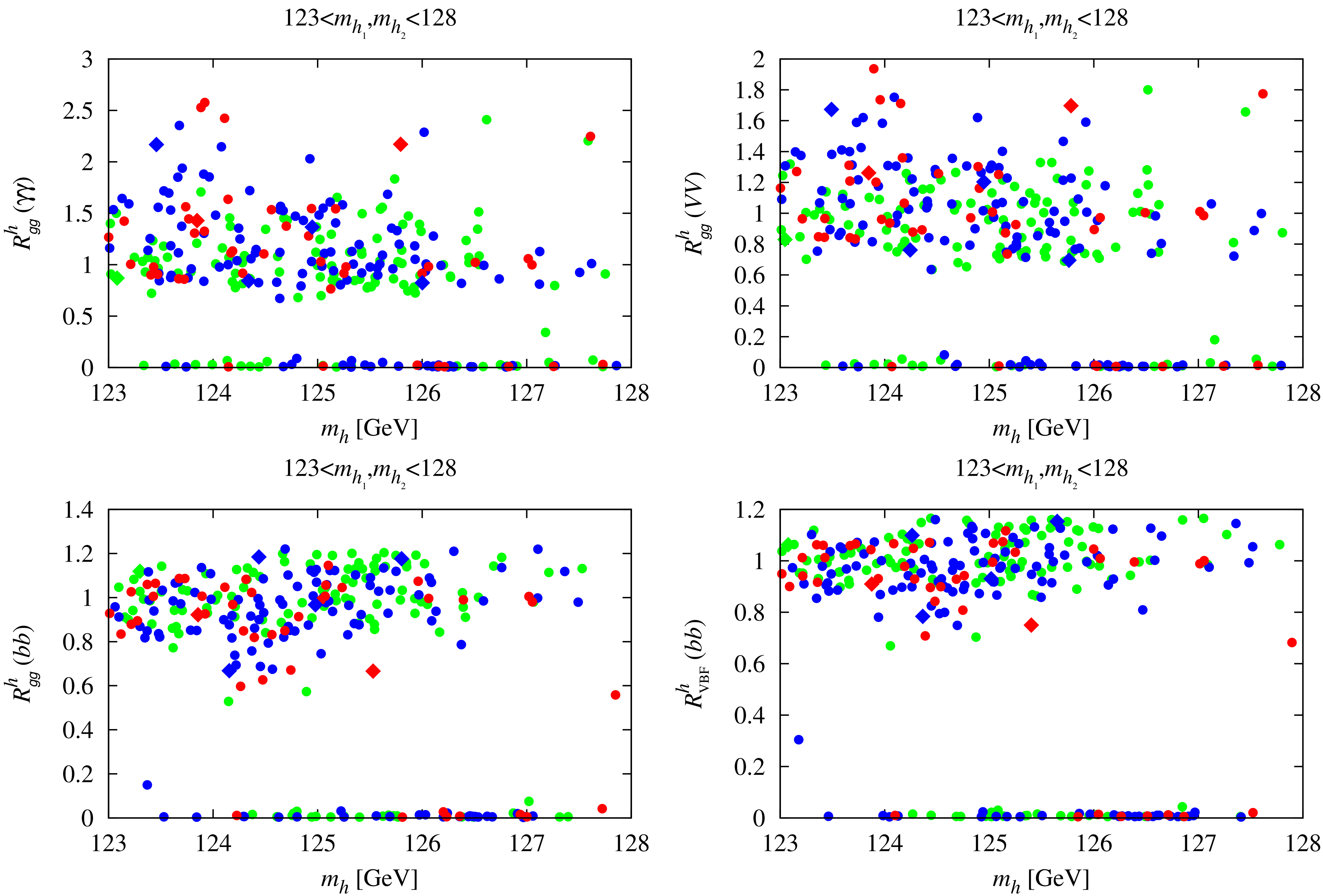

Figure 5: $R^h_{gg}(X)$ **for** $X = \gamma\gamma, VV, b\bar{b}$, **and** $R^h_{\rm VBF}(b\bar{b})$ **versus** m_h. **For application to the Tevatron, note that** $R^h_{\rm VBF}(b\bar{b}) = R^h_{W^*\to Wh}(b\bar{b})$.

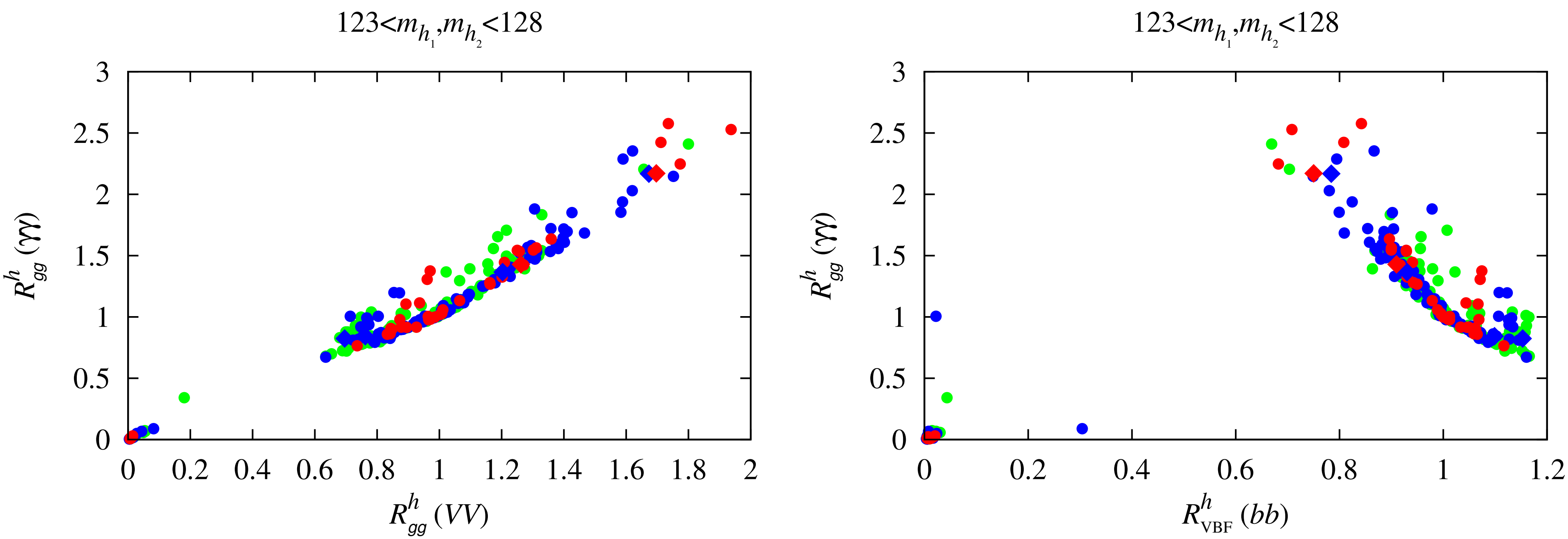

Figure 6: Left: correlation between the gluon fusion induced $\gamma\gamma$ and VV rates relative to the SM. Right: correlation between the gluon fusion induced $\gamma\gamma$ rate and the WW fusion induced $b\overline{b}$ rates relative to the SM; the relative rate for $W^* \to Wh$ with $h \to b\overline{b}$ (relevant for the Tevatron) is equal to the latter.

- **Comments on Fig. 6:**

  1. Left-hand plot shows the strong correlation between $R^h_{gg}(\gamma\gamma)$ and $R^h_{gg}(VV)$.

Note that if $R^h_{gg}(\gamma\gamma) \sim 1.5$, as suggested by current experimental results, then in this model $R^h_{gg}(VV) \geq 1.2$.

2. The right-hand plot shows the (anti) correlation between $R^h_{gg}(\gamma\gamma)$ and $R^h_{W^*\to Wh}(b\bar{b}) = R^h_{\rm VBF}(b\bar{b})$.
   In general, the larger $R^h_{gg}(\gamma\gamma)$ is, the smaller the value of $R^h_{W^*\to Wh}(b\bar{b})$.
   However, this latter plot shows that there *are* parameter choices for which both the $\gamma\gamma$ rate at the LHC and the $W^* \to Wh(\to b\bar{b})$ rate at the Tevatron (and LHC) can be enhanced relative to the SM as a result of there being contributions to these rates from both the h_1 and h_2.
3. It is often the case that one of the h_1 or h_2 dominates $R^h_{gg}(\gamma\gamma)$ while the other dominates $R^h_{W^*\to Wh}(b\bar{b})$. This is typical of the diamond WMAP-window points.
   However, a significant number of the circular $\Omega h^2 < 0.094$ points are such that either the $\gamma\gamma$ or the $b\bar{b}$ signal receives substantial contributions from both the h_1 and the h_2.
   We did not find points where the $\gamma\gamma$ and $b\bar{b}$ final states *both* receive substantial contributions from *both* the h_1 and h_2.

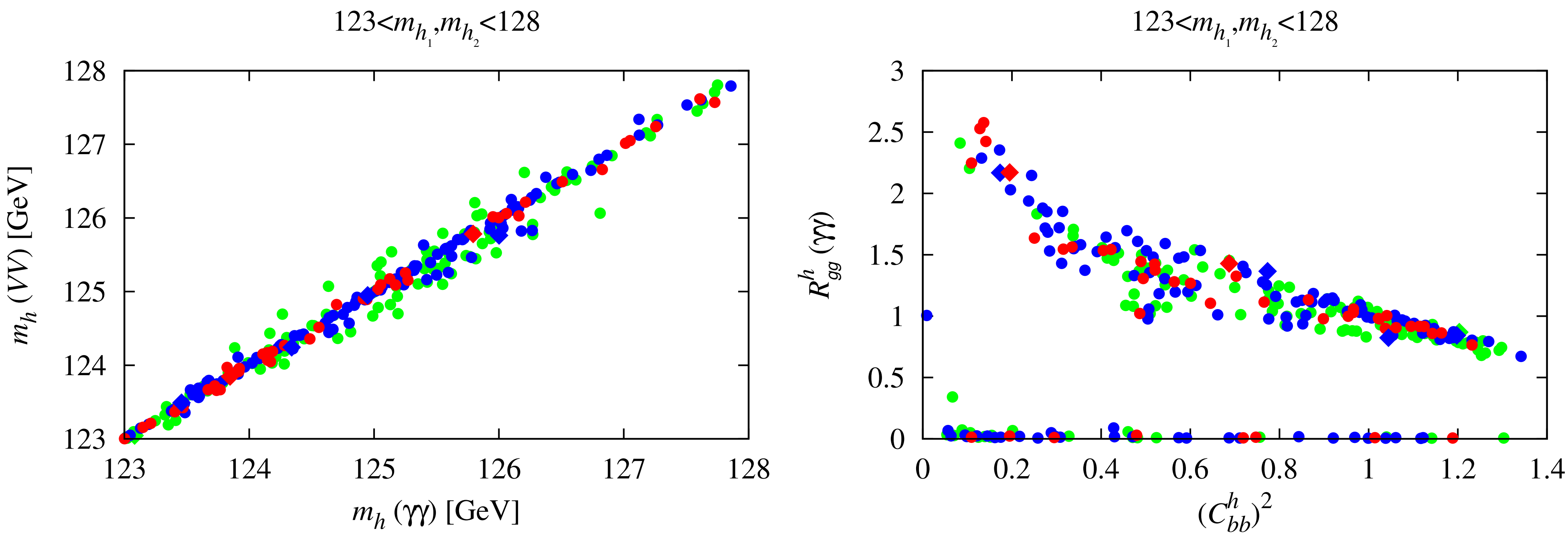

Figure 7: **Left: effective Higgs masses obtained from different channels: $m_h^{gg}(\gamma\gamma)$ versus $m_h^{gg}(VV)$. Right: $\gamma\gamma$ signal strength $R^h_{gg}(\gamma\gamma)$ versus effective coupling to $b\bar b$ quarks $(C^h_{b\bar b})^2$. Here, ${C^h_{b\bar b}}^2 \equiv \left[R^{h_1}_{gg}(\gamma\gamma){C^{h_1}_{b\bar b}}^2 + R^{h_2}_{gg}(\gamma\gamma){C^{h_2}_{b\bar b}}^2\right] / \left[R^{h_1}_{gg}(\gamma\gamma) + R^{h_2}_{gg}(\gamma\gamma)\right]$.**

Comments on Fig. 7

1. **The m_h values for the gluon fusion induced $\gamma\gamma$ and VV cases are also strongly correlated — in fact, they differ by no more than a fraction of a**

GeV and are most often much closer, see the left plot of Fig. 7.

2. The right plot of Fig. 7 illustrates the mechanism behind enhanced rates, namely that large net $\gamma\gamma$ branching ratio is achieved by reducing the average total width by reducing the average $b\bar{b}$ coupling strength.

- The dependence of $R^h_{gg}(\gamma\gamma)$ on λ, κ, $\tan\beta$ and $\mu_{\rm eff}$ is illustrated in Fig. 8.

  We observe that the largest $R^h_{gg}(\gamma\gamma)$ values arise at large λ, moderate κ, small $\tan\beta < 5$ (but note that $R^h_{gg}(\gamma\gamma) > 1.5$ is possible even for $\tan\beta = 15$) and small $\mu_{\rm eff} < 150~{\rm GeV}$.

  Such low values of $\mu_{\rm eff}$ are very favorable in point of view of fine-tuning, in particular if stops are also light.

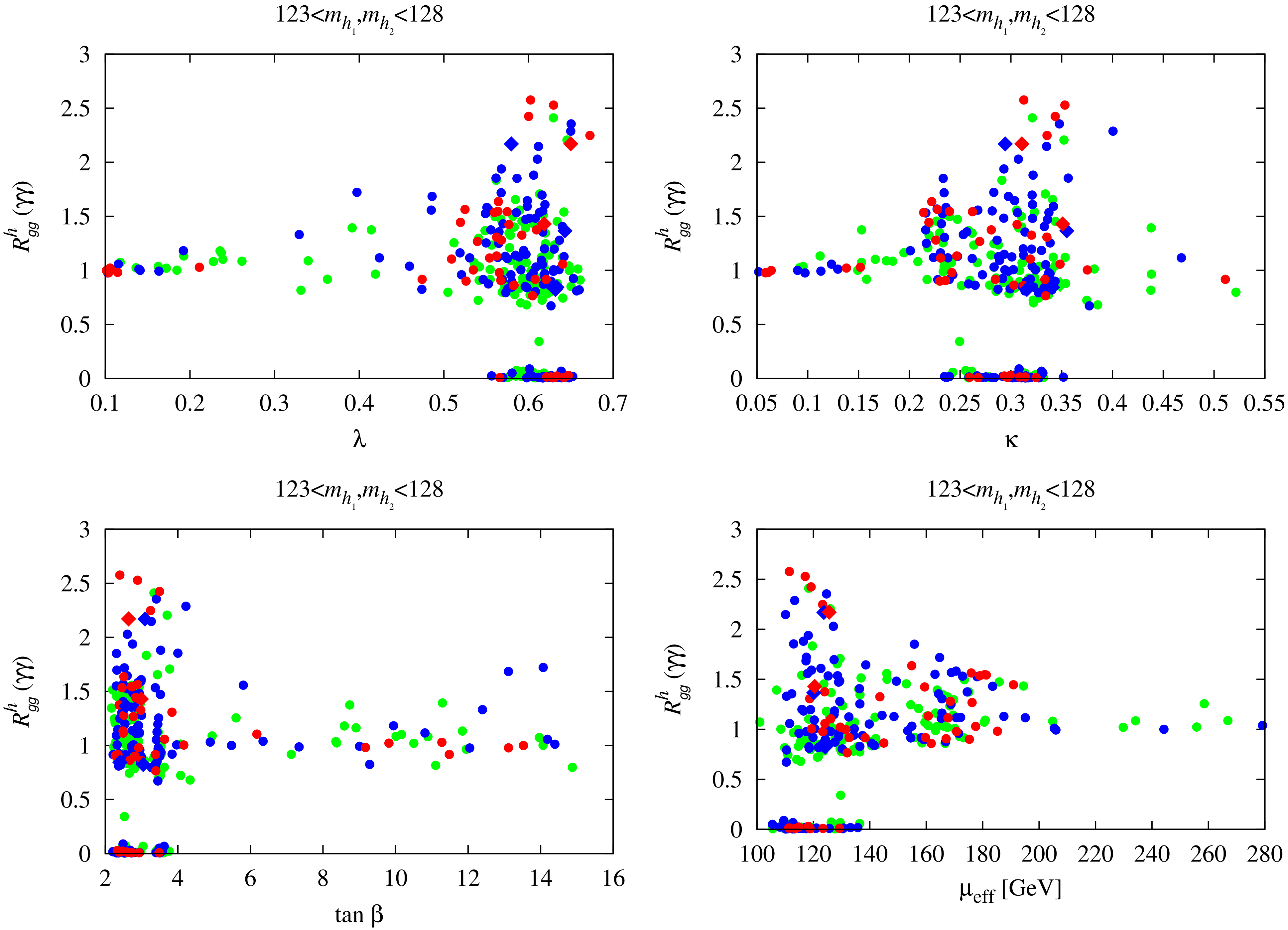

Figure 8: Dependence of $R^h_{gg}(\gamma\gamma)$ on λ, κ, $\tan\beta$ and $\mu_{\rm eff}$.

Fig. 9 shows that the stop mixing is typically large in these cases, $(A_t - \mu_{\rm eff}\cot\beta)/M_{\rm SUSY} \approx 1.5$–$2$. Moreover, the few points which we found in the WMAP window always have $m_{\tilde t_1} < 700~{\rm GeV}$.

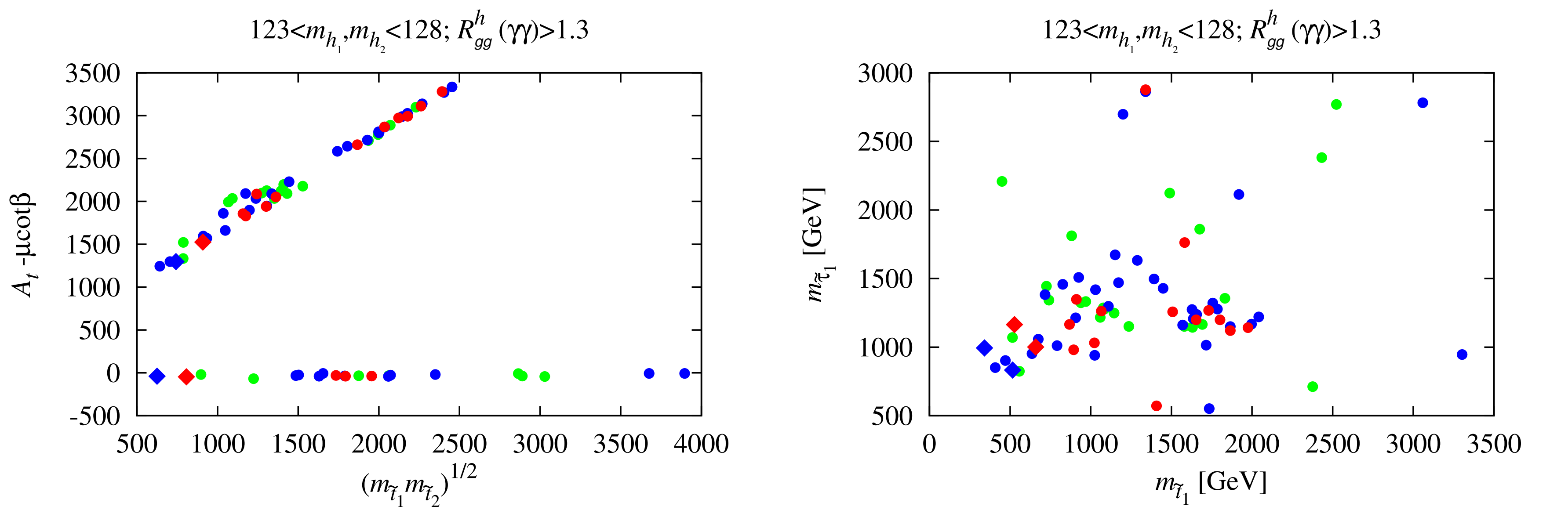

Figure 9: Left: Stop mixing parameter vs. $M_{\rm SUSY} \equiv \sqrt{m_{\tilde t_1} m_{\tilde t_2}}$. Right: $m_{\tilde\tau_1}$ vs. $m_{\tilde t_1}$. . Points plotted have $R^h_{gg}(\gamma\gamma) > 1.3$.

- Implications of the enhanced $\gamma\gamma$ rate scenarios for other observables are also quite interesting.

First, let us observe from Fig. 10 that these scenarios have squark and gluino masses that are above about 1.25 TeV ranging up to as high as 6 TeV (where our scanning more or less ended).

The WMAP-window points with large $R^h_{gg}(\gamma\gamma)$ are located at low masses of $m_{\widetilde g} \sim 1.3$ TeV and $m_{\widetilde q} \sim 1.6$ TeV.

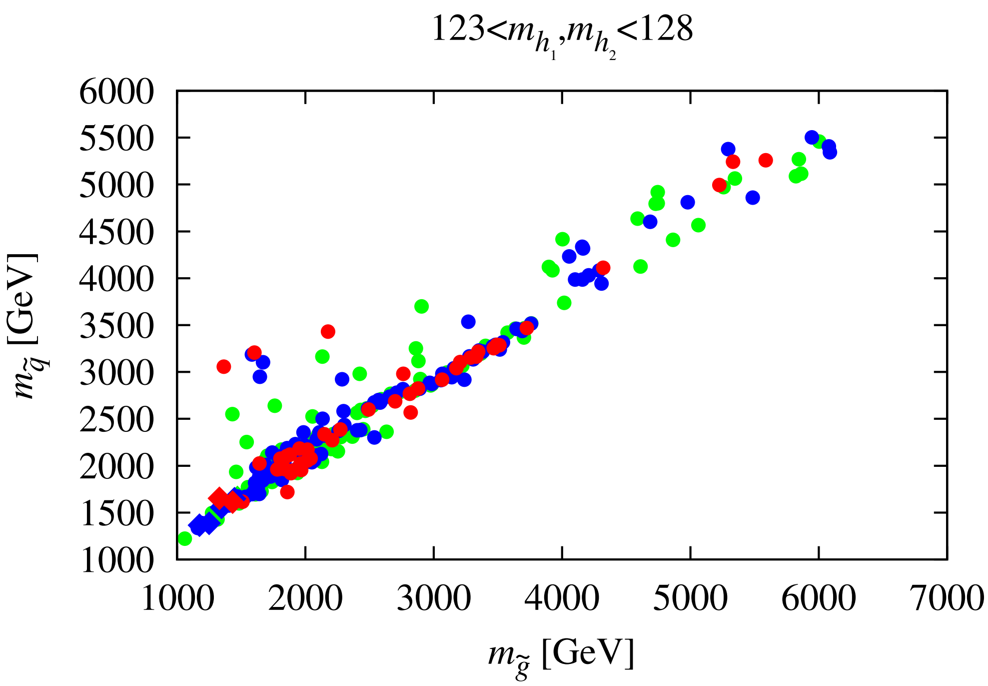

Figure 10: Average light-flavor squark mass, $m_{\widetilde q}$, versus gluino mass, $m_{\widetilde g}$, for the points plotted in the previous figures.

- The value of $R_{gg}^{h}(\gamma\gamma)$ as a function of the masses of the other Higgs bosons is illustrated in Fig. 11.

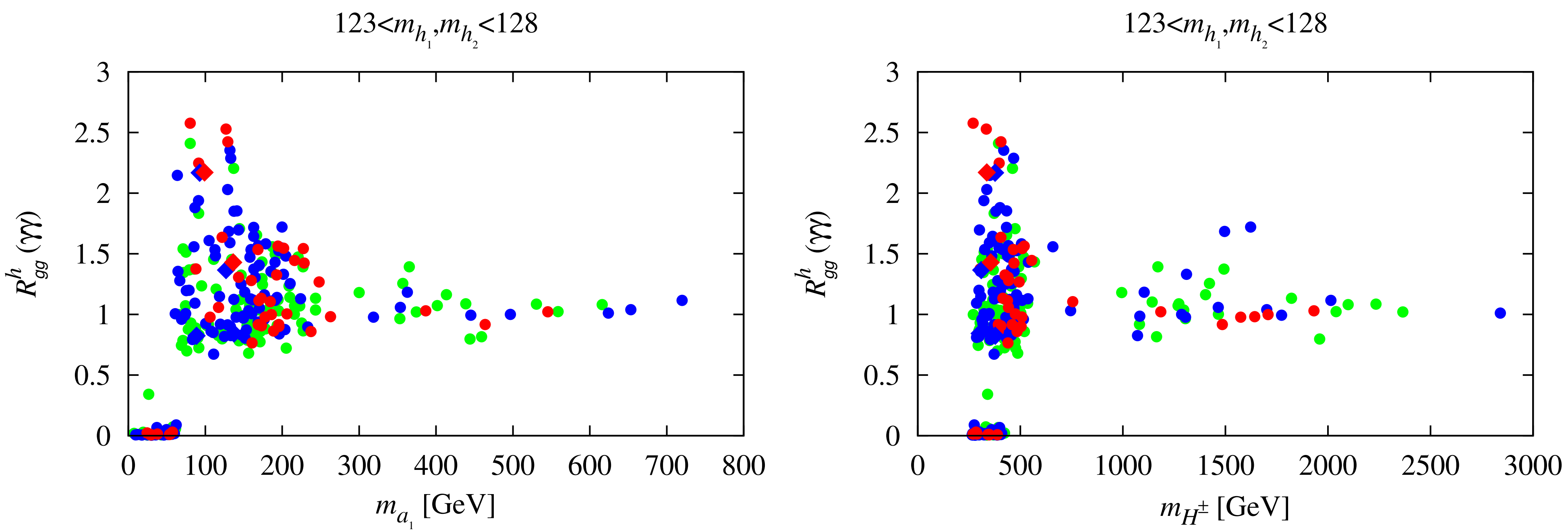

Figure 11: $R_{gg}^{h}(\gamma\gamma)$ versus the masses of m_{a_1} and $m_{H^\pm}$ (note that $m_{H^\pm} \simeq m_{a_2} \simeq m_{h_3}$).

Comments on Fig. 11:

1. We see that values above of $R^{h}(\gamma\gamma) > 1.7$ are associated with masses

for the a_2, h_3 and $H^\pm$ of order $\lesssim 500\ \mathrm{GeV}$ and for the a_1 of order $\lesssim 150\ \mathrm{GeV}$.
(Note that $m_{a_2} \simeq m_{h_3} \simeq m_{H^\pm}$)
While modest in size, detectability of these states at such masses requires further study.

2. One interesting point is that $m_{a_1} \sim 125\ \mathrm{GeV}$ is common for points with $R^h_{gg}(\gamma\gamma) > 1$ points.
   We have checked that $R^{a_1}_{gg}(\gamma\gamma)$ is quite small for such points — typically $\lesssim 0.01$.

- In Fig. 12, we display Ωh^2 and the spin-independent cross section for LSP scattering on protons, σ_{SI}, for the points plotted in previous figures.

  Comments on Fig. 12:

1. Very limited range of LSP masses consistent with the WMAP window, roughly $m_{\widetilde\chi^0_1} \in [60, 80]\ \mathrm{GeV}$.
2. Corresponding σ_{SI} values range from $few \times 10^{-9}\ \mathrm{pb}$ to as low as $few \times 10^{-11}\ \mathrm{pb}$.

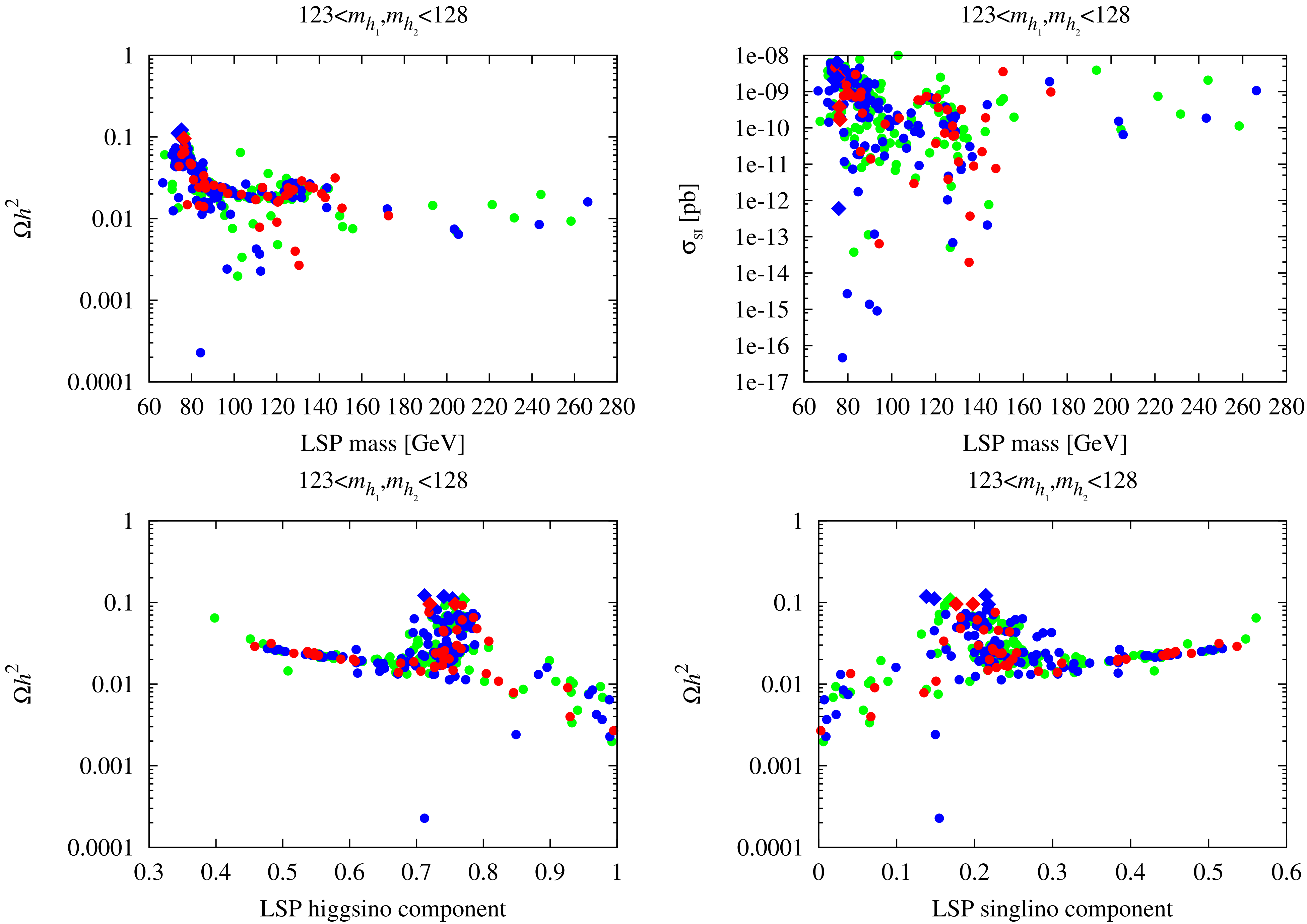

Figure 12: Top row: Ωh^2 and spin-independent cross section on protons versus LSP mass for the points plotted in previous figures. Bottom row: Ωh^2 versus LSP higgsino (left) and singlino (right) components.

3. Owing to the small $\mu_{\rm eff}$, the LSP is dominantly higgsino, which is also the reason for Ωh^2 typically being too low.
   The points with Ωh^2 within the WMAP window are mixed higgsino–singlino, with a singling component of the order of 20%, see the bottom-row plots of Fig. 12.

- It is interesting to note a few points regarding the parameters associated with the points plotted in previous figures.

1. For the WMAP-window diamond points,$\lambda \in [0.58, 0.65]$, $\kappa \in [0.28, 0.35]$, and $\tan\beta \in [2.5, 3.5]$.
2. Points with $R^h_{gg}(\gamma\gamma) > 1.3$ have $\lambda \in [0.33, 0.67]$, $\kappa \in [0.22, 0.36]$, and $\tan\beta \in [2, 14]$.

- Can't find scenarios of this degenerate/enhanced type such that δa_μ is consistent with that needed to explain the current discrepancy.

  In particular, the very largest value of δa_μ achieved is of order 1.8×10^{-10} and, further, the WMAP-window points with large $R^h_{gg}(\gamma\gamma, VV)$ have $\delta a_\mu < 6 \times 10^{-11}$.

- **How fine-tuned (in λ and κ) are the degenerate scenarios?**

A case where h_1 and h_2 share in producing a moderately enhanced $R^h(\gamma\gamma)$ maximum of ~ 1.2.

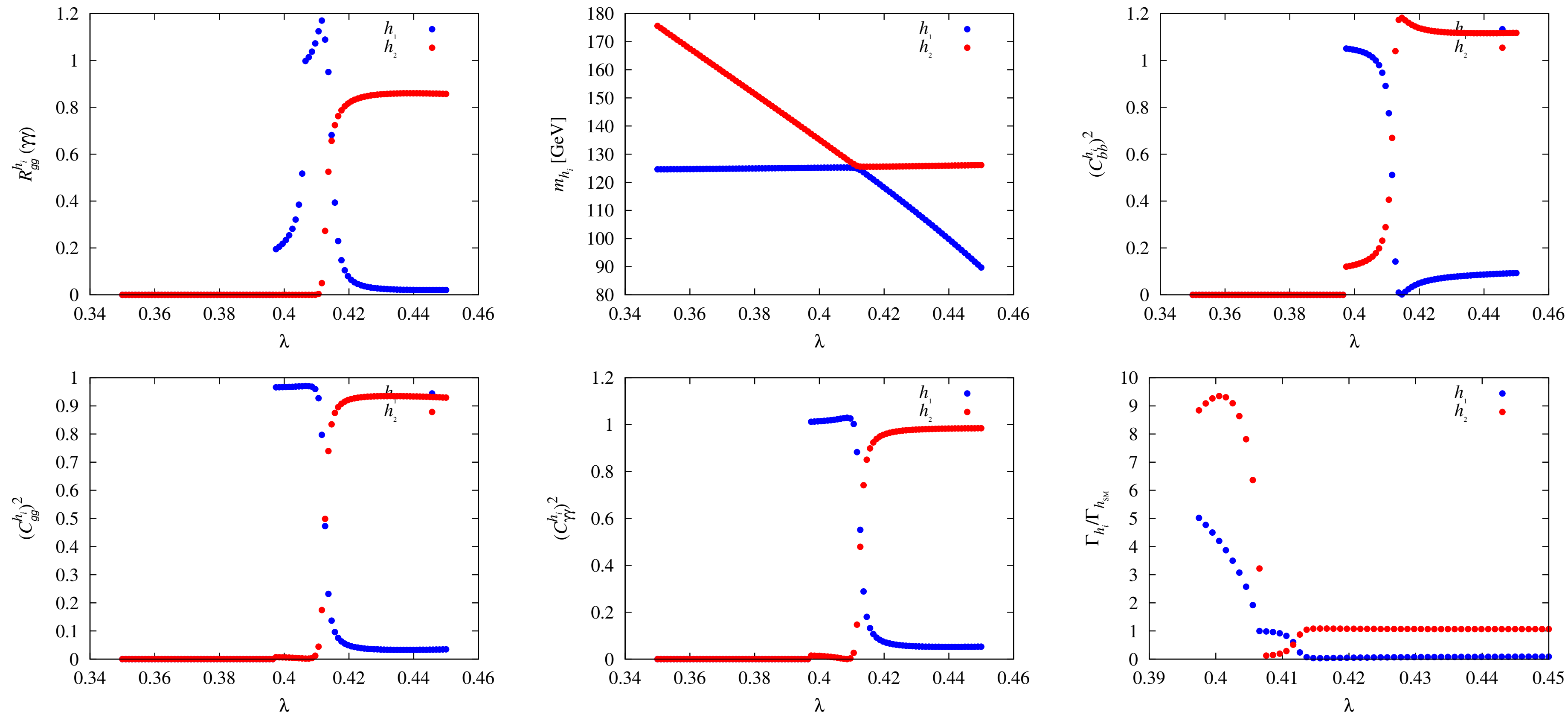

We see a modest interval in λ where the net $R^h(\gamma\gamma) \sim 1.2$ result is due to sharing.

A case where there is a sharp switchover from h_1 to h_2 and only close coincidence leads to very enhanced $R^h(\gamma\gamma)$ maximum of ~ 2.5.

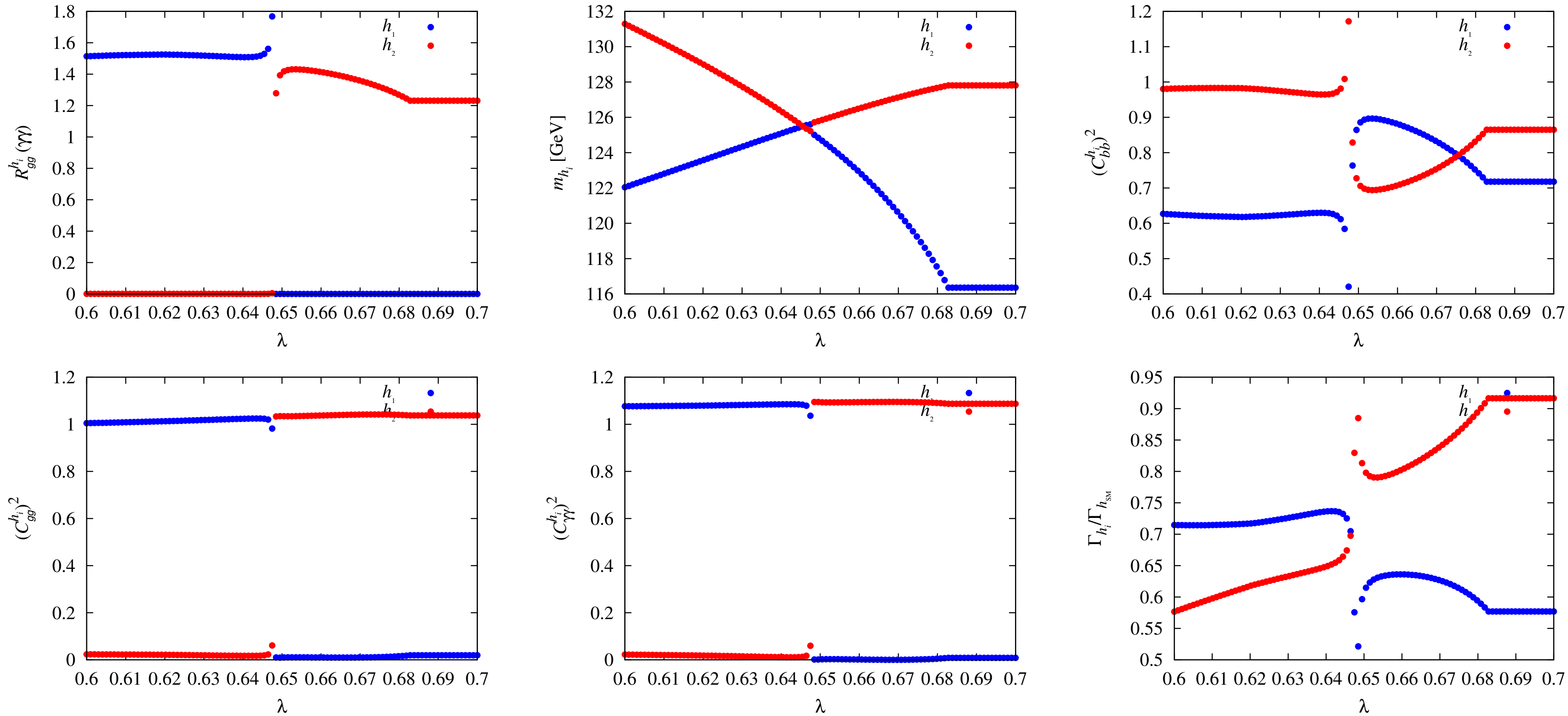

There is a much smaller interval in λ where large $R^h(\gamma\gamma)$ is achieved.

Conclusions

- It seems likely that the Higgs responsible for EWSB has emerged.
- Perhaps, other Higgs-like objects are emerging.
- Survival of enhanced signals for one or more Higgs boson would be one of the most exciting outcomes of the current LHC run and would guarantee years of theoretical and experimental exploration of BSM models with elementary scalars.
- $>$SM signals would appear to guarantee the importance of a linear collider in order to understand fully the responsible BSM physics.
- In any case, the current situation illusrates the fact that we must never assume we have uncovered all the Higgs.

Certainly, I will continue watching and waiting

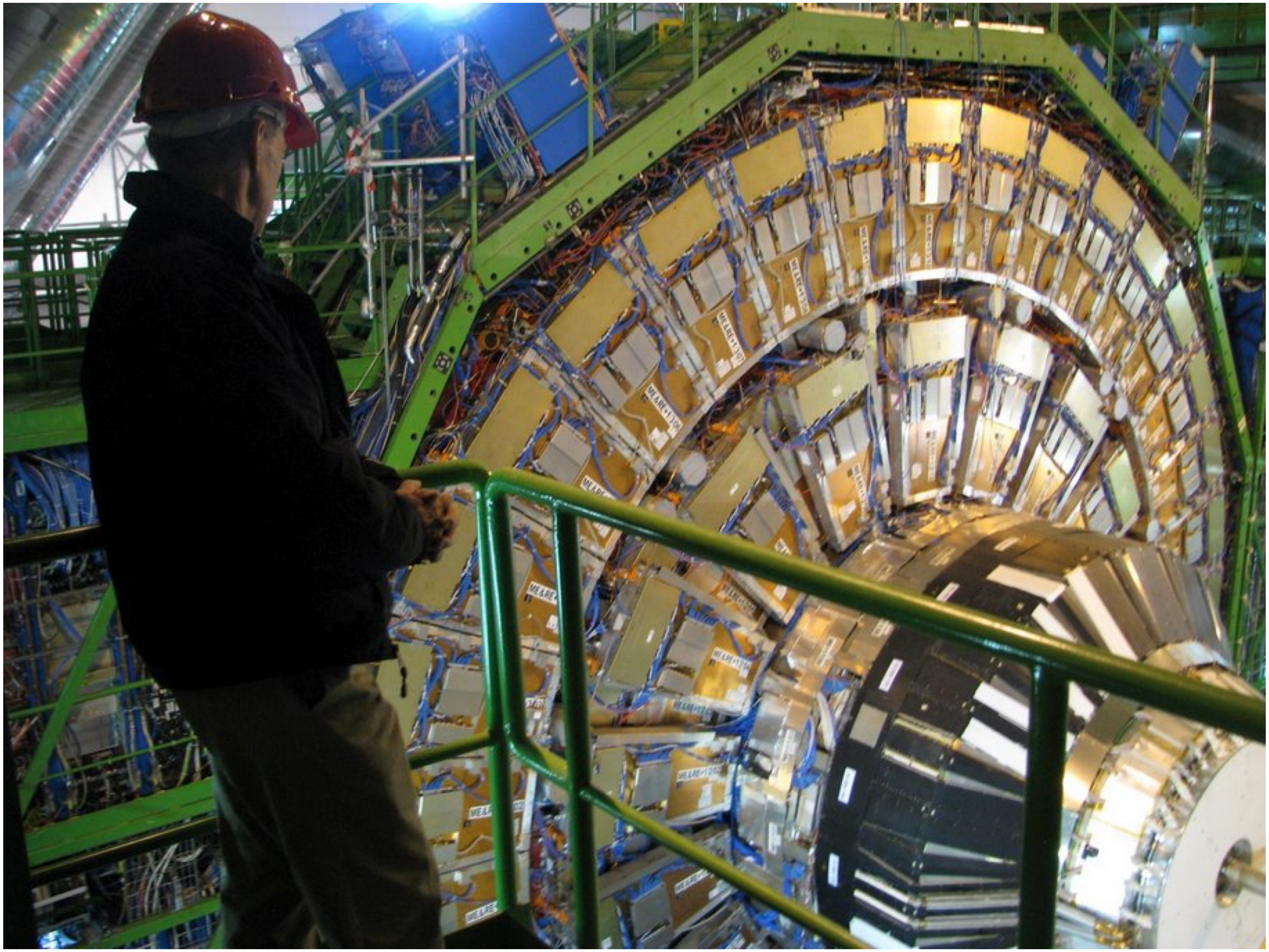

References

[1] J. F. Gunion, Y. Jiang and S. Kraml, arXiv:1201.0982 [hep-ph].

[2] U. Ellwanger, arXiv:1112.3548 [hep-ph].

[3] L. Randall and R. Sundrum, “A large mass hierarchy from a small extra dimension,” Phys. Rev. Lett. 83 (1999) 3370 [arXiv:hep-ph/9905221];

[4] H. Davoudiasl, J. L. Hewett and T. G. Rizzo, Phys. Lett. B 473, 43 (2000) [hep-ph/9911262].

[5] A. Pomarol, Phys. Lett. B 486, 153 (2000) [hep-ph/9911294].

[6] T. Gherghetta, A. Pomarol, “Bulk fields and supersymmetry in a slice of AdS,” Nucl. Phys. B586, 141-162 (2000). [hep-ph/0003129].

[7] H. Davoudiasl, J. L. Hewett, T. G. Rizzo, Phys. Rev. D63, 075004 (2001). [hep-ph/0006041].

[8] C. Csaki, J. Erlich and J. Terning, Phys. Rev. D 66, 064021 (2002) [hep-ph/0203034].

[9] J. L. Hewett, F. J. Petriello and T. G. Rizzo, JHEP 0209, 030 (2002) [hep-ph/0203091].

[10] K. Agashe, A. Delgado, M. J. May and R. Sundrum, JHEP 0308, 050 (2003) [hep-ph/0308036].

[11] K. Agashe, H. Davoudiasl, G. Perez and A. Soni, Phys. Rev. D 76, 036006 (2007) [hep-ph/0701186].

[12] D. Dominici, B. Grzadkowski, J. F. Gunion and M. Toharia, "The scalar sector of the Randall-Sundrum model," Nucl. Phys. B 671, 243 (2003) [arXiv:hep-ph/0206192]; "Higgs-boson interactions within the Randall-Sundrum model," Acta Phys. Polon. B 33, 2507 (2002) [arXiv:hep-ph/0206197].

[13] G. Cacciapaglia, C. Csaki, J. Galloway, G. Marandella, J. Terning and A. Weiler, JHEP 0804, 006 (2008) [arXiv:0709.1714 [hep-ph]].

[14] K. Agashe, A. Belyaev, T. Krupovnickas, G. Perez and J. Virzi, Phys. Rev. D 77, 015003 (2008) [hep-ph/0612015].

[15] G. Aad *et al.* **[ATLAS Collaboration], arXiv:1112.2194 [hep-ex].**

[16] S. Chatrchyan *et al.* **[CMS Collaboration], arXiv:1112.0688 [hep-ex].**

[17] S. Rappoccio [CMS Collaboration], arXiv:1110.1055 [hep-ex].

[18] The ATLAS Collaboration, " A Search for ttbar Resonances in the Dilepton Channel in 1.04/fb of pp Collisions at sqrt(s) = 7 TeV", ATLAS-CONF-2011-123.

[19] G. F. Giudice, R. Rattazzi and J. D. Wells, "Graviscalars from higher-dimensional metrics and curvature-Higgs mixing," Nucl. Phys. B 595, 250 (2001) [arXiv:hep-ph/0002178].

[20] J. L. Hewett and T. G. Rizzo, JHEP 0308, 028 (2003) [hep-ph/0202155].

[21] C. Csaki, J. Hubisz, S. J. Lee, "Radion phenomenology in realistic warped space models," Phys. Rev. D76, 125015 (2007). [arXiv:0705.3844 [hep-ph]].

[22] H. de Sandes, R. Rosenfeld, "Radion-Higgs mixing effects on bounds from LHC Higgs Searches," [arXiv:1111.2006 [hep-ph]].

[23] V. Barger, M. Ishida, "Randall-Sundrum Reality at the LHC," [arXiv:1110.6452 [hep-ph]].

[24] K. Cheung and T. -C. Yuan, arXiv:1112.4146 [hep-ph].

[25] V. Barger, M. Ishida and W. -Y. Keung, arXiv:1111.4473 [hep-ph].

[26] ATLAS Collaboration, Combination of Higgs Boson Searches with up to 4.9 fb^{-1} of pp Collisions Data Taken at a center-of-mass energy of 7 TeV with the ATLAS Experiment at the LHC, ATLAS-CONF-2011-163.

[27] CMS Collaboration, Combination of SM Higgs Searches, CMS-PAS-HIG-11-032.

[28] ATLAS Collaboration, Search for the Standard Model Higgs boson in the decay channel $H \to ZZ^{(*)} \to 4\ell$ at $\sqrt{s} = 7$ TeV.

[29] CMS Collaboration, Search for a Higgs boson produced in the decay channel 4l, CMS-PAS-HIG-11-025.

[30] H. Baer, V. Barger and A. Mustafayev, Implications of a 125 GeV Higgs scalar for LHC SUSY and neutralino dark matter searches, arXiv:1112.3017.

[31] A. Arbey, M. Battaglia, A. Djouadi, F. Mahmoudi, J. Quevillon, Implications of a 125 GeV Higgs for supersymmetric models, arXiv:1112.3028.

[32] A. Arbey, M. Battaglia, F. Mahmoudi, Constraints on the MSSM from

the Higgs Sector - A pMSSM Study of Higgs Searches, $B_s \to \mu^+\mu^-$ and Dark Matter Direct Detection, arXiv:1112.3032.

[33] M. Carena, S. Gori, N. R. Shah, C. E. Wagner, A 125 GeV SM-like Higgs in the MSSM and the $\gamma\gamma$ rate, arXiv:1112.3336.

[34] O. Buchmueller, R. Cavanaugh, A. De Roeck, *et al.*, Higgs and Supersymmetry, arXiv:1112.3564 [hep-ph].

[35] S. Akula, B. Altunkaynak, D. Feldman, P. Nath, G. Peim, Higgs Boson Mass Predictions in SUGRA Unification, Recent LHC-7 Results, and Dark Matter, arXiv:1112.3645.

[36] M. Kadastik, K. Kannike, A. Racioppi, M. Raidal, Implications of 125 GeV Higgs boson on scalar dark matter and on the CMSSM phenomenology, arXiv:1112.3647.

[37] J. Cao, Z. Heng, D. Li, J. M. Yang, Current experimental constraints

on the lightest Higgs boson mass in the constrained MSSM, arXiv:1112.4391.

[38] A. Arvanitaki, G. Villadoro, A Non Standard Model Higgs at the LHC as a Sign of Naturalness, arXiv:1112.4835.

[39] L. J. Hall, D. Pinner, J. T. Ruderman, A Natural SUSY Higgs Near 126 GeV, arXiv:1112.2703.

[40] U. Ellwanger, A Higgs boson near 125 GeV with enhanced di-photon signal in the NMSSM, arXiv:1112.3548.

[41] A. Djouadi, U. Ellwanger and A. M. Teixeira, The Constrained next-to-minimal supersymmetric standard model, Phys. Rev. Lett. 101 (2008) 101802, arXiv:0803.0253.

[42] A. Djouadi, U. Ellwanger and A. M. Teixeira, Phenomenology of the constrained NMSSM, JHEP 0904 (2009) 031 arXiv:0811.2699.

[43] U. Ellwanger, J. F. Gunion, C. Hugonie, NMHDECAY: A Fortran code for the Higgs masses, couplings and decay widths in the NMSSM, JHEP 0502 (2005) 066, arXiv:hep-ph/0406215.

[44] U. Ellwanger, C. Hugonie, NMHDECAY 2.0: An Updated program for sparticle masses, Higgs masses, couplings and decay widths in the NMSSM, Comput. Phys. Commun. 175 (2006) 290–303, arXiv:hep-ph/0508022.

[45] http://www.th.u-psud.fr/NMHDECAY/nmssmtools.html.

[46] A. Djouadi, J. Kalinowski, M. Spira, HDECAY: A Program for Higgs boson decays in the standard model and its supersymmetric extension, Comput.Phys.Commun. 108 (1998) 56–74, arXiv:hep-ph/9704448.

[47] R. Dermisek, J. F. Gunion, The NMSSM Close to the R-symmetry Limit and Naturalness in $h \to aa$ Decays for $m_a < 2m_b$, Phys. Rev. D75 (2007) 075019, arXiv:hep-ph/0611142.

[48] B. A. Dobrescu, K. T. Matchev, Light axion within the next-to-minimal supersymmetric standard model, JHEP 0009 (2000) 031, arXiv:hep-ph/0008192.

[49] J. Incandela, F. Gianotti, “Latest update in the search for the Higgs boson”, CERN seminar on 4 July 2012, http://indico.cern.ch/conferenceDisplay.py?confId=197461.

[50] http://www.atlas.ch/news/2012/latest-results-from-higgs-search.html.

[51] http://cms.web.cern.ch/news/observation-new-particle-mass-125-gev.

[52] [TEVNPH Working Group], Updated Combination of CDF and D0 Searches for Standard Model Higgs Boson Production with up to $10\ \mathbf{fb}^{-1}$ of Data, see http://www.fnal.gov/pub/presspass/press_releases/2012/Higgs-Tevatron-20120702.html.

[53] J. F. Gunion, Y. Jiang and S. Kraml, The Constrained NMSSM and Higgs near 125 GeV, Phys. Lett. B 710, 454 (2012), arXiv:1201.0982[hep-ph].

[54] U. Ellwanger and C. Hugonie, Higgs bosons near 125 GeV in the NMSSM with constraints at the GUT scale, arXiv:1203.5048[hep-ph].

[55] U. Ellwanger, A Higgs boson near 125 GeV with enhanced di-photon signal in the NMSSM, JHEP 1203 (2012) 044, arXiv:1112.3548[hep-ph].

[56] U. Ellwanger, J. F. Gunion, C. Hugonie, NMHDECAY: A Fortran code for the Higgs masses, couplings and decay widths in the NMSSM, JHEP 0502 (2005) 066, arXiv:hep-ph/0406215.

[57] U. Ellwanger, C. Hugonie, NMHDECAY 2.0: An Updated program for sparticle masses, Higgs masses, couplings and decay widths in the NMSSM, Comput. Phys. Commun. 175 (2006) 290–303, arXiv:hep-ph/0508022.

[58] http://www.th.u-psud.fr/NMHDECAY/nmssmtools.html.

[59] **E. Aprile** *et al.* **[XENON100 Collaboration], Dark Matter Results from 100 Live Days of XENON100 Data, Phys. Rev. Lett. 107, 131302 (2011),** arXiv:1104.2549[astro-ph.CO].

[60] **S. Chatrchyan** *et al.* **[CMS Collaboration], Search for the standard model Higgs boson decaying into two photons in pp collisions at sqrt(s)=7 TeV, Phys. Lett. B 710, 403 (2012),** arXiv:1202.1487[hep-ex].